BRAC University Journal, Vol. X, No. 1 & 2, 2013, pp. 13-29

ON TERAHERTZ LASER PULSE PROPAGATION IN NEGATIVE INDEX METAMATERIALS

U. A. Mofiz[1]
Plasma Astrophysics Laboratory
Department of Mathematics and Natural Science
BRAC University, 66 Mohakhali
Dhaka-1212, Bangladesh
email: mofiz@bracu.ac.bd

ABSTRACT

The nonlinear propagation of a terahertz laser pulse propagation in the resonant region of a negative index meta-material is investigated. The resonant frequency of a split ring resonator (SRR), comprosing the negative index metamaterial, is calculated to be in the order of terahertz. The analysis shows that the negative refractive index in SRR is maintained within a narrow band of the frequency, which is more narrowed down with the intensity of the laser radiation. From Maxwell's system of equations, a system of coupled equations descring the nonlinear propagation of laser pulse in negative index metamaterials is obtained. The system of the coupled equations are solved analytically in the high frequency and in the low frequency responses. In the high frequency response, a nonlinear field dependent dispersion relation is obtained, and the corresponding group velocity is determined. In the low frequency response, introducing the Lorentz invariant stretched coordinates, a system of coupled nonlinear Schrödinger equations (NLSE) are obtained. Considering the equal intensities of electric and magnetic fields of the laser pulse, the coupled NLSE equations are solved , which shows that the laser radiation creates bright and dark optical solitons, respectively, before and after a critical frequency, within the narrow band, determined by the intensity of the laser radiation. The instability of the bright soliton is investigated while the dark soliton is modulationally stable.

Key words: meta-material; negative refractive index; bright and dark solitons.

I. INTRODUCTION

I.1. History of Negative Index Metamaterials

Vaselago [1], a Russian physicist in 1967 hypothetically studied the optical properties of an isotropic medium with simultaneously negative electric permittivity (ε) and magnetic permeability (μ), which he named a left- handed material (LHM). He showed LHMs display unique "reversed" electromagnetic (EM) properties having the triad $\vec{k}$ (wave vector), $\vec{E}$ (electric field), $\vec{H}$ (magnetic field) left handed, hence exhibiting phase and energy velocities of opposite directions. A LHM is characterized by negative refractive index n, therefore, their alternative name, negative index materials (NIMs). Such materials demonstrate a number of peculiar properties: reversal of Snell's law of refraction, reversal of the Doppler shift, counterdirected Cherenkov radiation cone, the refocusing of EM waves from a point source, etc.

The remarkable property of a LHM is that it possees a negative refractive index due to which a thin negative index film will behave as a "superlens", providing image detail with a resolution beyond the diffraction limit. Conventional positive index lenses require curved surface to bent the rays coming from an object to form an image but in the case of negative refractive index a planar slab can produce image within the slab and also outside the slab (Fig.1).

1. For all correspondence

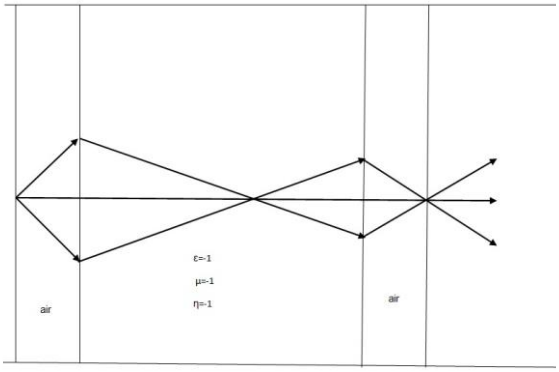

Fig.1. A negative n medium bends light to a negative angle relative to the surface normal. Light formerly diverging from a point source, converged back within the metamaterial as well as second time in the image plane outside.

Pendry[2] carefully rexamined the plannar lense and found that it may recover the evanescent waves coming from an object. In a planar negative index lense, an evanesciting wave decaying away from an object grows exponentially in the lens and deacys agin until it reaches the image plane (Fig.2).

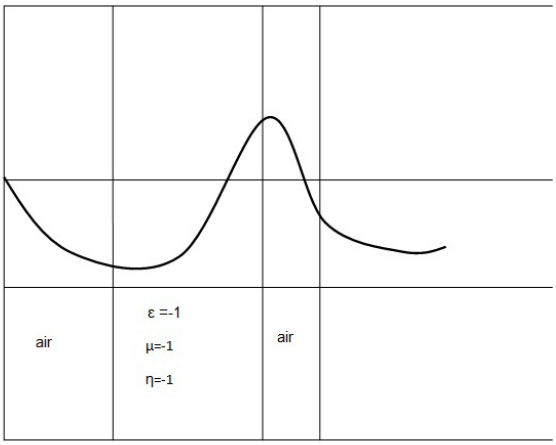

Fig.2. A decaying wave grows exponentially within the metamaterial and then decays again utside.

Vaselago's idea remains hypothetical for a long time, untill a breakthrough was announced in 2000 by Smith and co-workers [3] presented evidence for a composite material of conducting rings and wires – called split ring resonator (SRR)-displaying the negative value of ε and μ. The SRR structure has proven a remarkably efficient means of producing a magnetic response by scaling down the size thus upwards in frequency to produce metamaterials in the terahertz frequencies [4]. Negative refraction in photonic crystal is also feasible [5] in doped graphene metamaterials .

I.2. Negative Refraction in Photonic Crystals

Photonic crystals (PCs) are made only from dielectrics, thus smaller losses than metalic LHMs, especially at high frequencies. In PCs, to achieve negative refraction the size and periodicity of the "atoms" (the elimentary units) are of the order of the wave length. In PCs, no effective ε and μ can be defined, although the phase and energy velocity can be opposite as in the case in normal LHMs. Both negative refraction and superlensing have observed in PCs [6]. An alternative approach for fabricating metamaterial is to use PCs composed of polartonic materials [7].

I.3. Graphene Doped Metamaterials

Graphene is a two-dimensional , one atom thick allotrope of carbon holds the promise for building advanced nano-electronic devices since its discovery in 2004 [8]. It exhibits very unique optical properties, especially in the terahertz (THz) frequency range. To date, novel photonic devices such as THz devices, optical modulators, photodetectors, and polarizers were successfully realised. The physics of graphene can be considered as a unifying bridge between low-energy condensed matter physics and quantum field theory , as its two-dimensional quasi-electrons behaves like massless "relativistic" Dirac fermions, very similarly to electrically charged "neutrinos"[9].

Currently, the huge unexplored potential of graphene for nonlinear optics has been outlined. Strong nonlinear optical responses have investigated in papers [10,11]. Preliminary experimental include ultrafast saturable absorption and the observation of strong four wave mixing [12], which are the building blocks of nonlinear optics. This discoveries and the advancement in optical communications are the motivations to investigate the nonlinear propagation of intense terahertz laser pulse in meta-materials in the resonant region.

In this paper, we have investigated the nonlinear propagation of terahertz laser pulse in the resonant region of a negative index meta-material. The laser pulse is considered as the circularly polarized electromagnetic (EM) wave. In section II, we have

studied the optical properties of negative index meta-materials under EM fields and analyzed the nonlinear resonant frequency of the SRR. In section III, following Maxwell system equations, coupled equations for the complex electric field $\tilde{E}$ and the complex magnetic field $\tilde{H}$ are obtained, which are solved analytically in the high frequency as well as the low frequency responses. In the high frequency response, a nonlinear field dependent dispersion relation is obtained, which is analyzed with the increased field intensities. In the low frequency response, coupled nonlinear Schrödinger equations are obtained, the analysis of which shows that bright and dark optical solitons may propagate through NIMs within the frequency band, below and after some critical frequency, which is defined by the intensities of the wave fields. The bright soliton is modulationally unstable, its growth rate is calculated, while the dark soliton is modulationally stable. Results and discussions are given in section IV, while section V concludes the paper.

II. OPTICAL PROPERTIES OF NEGATIVE-INDEX MATERIALS UNDER ELECTROMAGNETIC FIELDS

II.1. Drude-Lorentz Form for Linear Dielectric Permittivity and Magnetic Permeability

The Drude-Lorentz forms for dielectric permittivity and magnetic permeability describe the EM response of materials over the high ranges of frequencies which are given by [13]:

$$\varepsilon = \varepsilon_0\left(1-\frac{\omega_{pe}^2}{\omega^2-\omega_{0e}^2+i\Gamma_e\omega}\right), \quad (1)$$

$$\mu = \mu_0\left(1-\frac{\omega_{pm}^2}{\omega^2-\omega_{0m}^2+i\Gamma_m\omega}\right), \quad (2)$$

where, ε_0 and μ_0 are the vacuum permittivity and permeability, respectively, with $\varepsilon_0\mu_0 = 1/c^2$; ω_{pe} and ω_{pm} are the electron /magnetic plasma frequency, ω_{0e} and ω_{0m} are the electron / magnetic resonant frequency, Γ_e and Γ_m are the electron/ magnetic damping coefficient and ω is the frequency of the EM wave. The free electron contribution in metals corresponds to $\omega_{0e} = 0$. Meta materials based on strong artificial resonant elements can also be described efficiently with the Drude-Lorentz formulas. These structures are the metallic wire structure which provides a predominently free-elctron respone to EM fields and the SRR structure provides a predominently magnetic response to EM fields.

II.2. Nonlinear Form of Dielectric Permittivity and Magnetic Permeability

The dielectric and the magnetic nonlinear responses of NIMs under EM fields without losses are given by the dispersive (frequency dependent) and the nonlinear (field dependent) expressions as [14]:

$$\varepsilon = \varepsilon_L(\omega) + \varepsilon_{NL}\left(\omega;|E|^2\right), \quad (3)$$

$$\mu = \mu_L(\omega) + \mu_{NL}\left(\omega;|H|^2\right), \quad (4)$$

where,

$$\varepsilon_L = \varepsilon_0\left(1-\omega_p^2/\omega^2\right), \quad (5)$$

$$\mu_L = \mu_0\left[1-F\omega^2/\left(\omega^2-\omega_0^2\right)\right]. \quad (6)$$

Under weak fields approximation:

$$\varepsilon_{NL} = \varepsilon_0\alpha\,|E|^2/E_c^2, \quad (7)$$

$$\mu_{NL} = \mu_0\beta\,|H|^2/E_c^2. \quad (8)$$

Here, ω_p is the plasma frequency, $F << 1$ is the filling factor, ω_0 is the linear resonant frequency, E_c is the critical electric field, $\alpha = 1$ corresponds to a focusing dielectric and $\alpha = -1$ corresponds to a defocusing dielectric, $\beta > 0$ is a fitting parameter.

II.3. Analysis of the Linear Response

The eigenfrequency of the system of SRRs in the linear limit is defined as [15]:

$$\omega_0 = (c/a_s)\sqrt{d_g/\pi h\varepsilon_{D0}}, \quad (9)$$

where, d_g is the size of the SRR gap, h is the width of the ring, a_s is the radius and c is the speed of light. ε_{D0} is the linear part of the dielectric. As per Ref. [15] for $\varepsilon_{D0} = 12.8$, $h = 0.003$ cm, $d_g = 0.1$ cm, $a_s = 0.003$ cm,

$c = 3\times10^{10}$ cm s^{-1}, we find $\omega_0 = 9.1\times10^{12}$ s^{-1} i.e the linear frequency $f_0 = \omega_0/2\pi = 1.45\times10^{12}$ Hz $= 1.45$ THz. For simultaneous $\varepsilon_L < 0$, $\mu_L < 0$, and $n = -\sqrt{\varepsilon_L\mu_L/\varepsilon_0\mu_0}$, we find $\omega_0 < \omega <$ min $\{\omega_p, \omega_M\}$, which corresponds $f_0 < f <$ min $\{f_p . f_M\}$. Here, $\omega_M = \omega_0/\sqrt{1-F^2}$. For $F = 0.4$; we find $f_M = 1.87$ THz; then, 1.45 THz $< f < 1.87$ THz. Considering $\omega_p = 2\pi\times10$ THz and $\omega_0 = 2\pi\times1.45$ THz, we plot ε, μ and n as functions of frequency within the frequency band 1.45THz $< f < 1.87$ THz , which are shown in FIG.3-5, respectively.

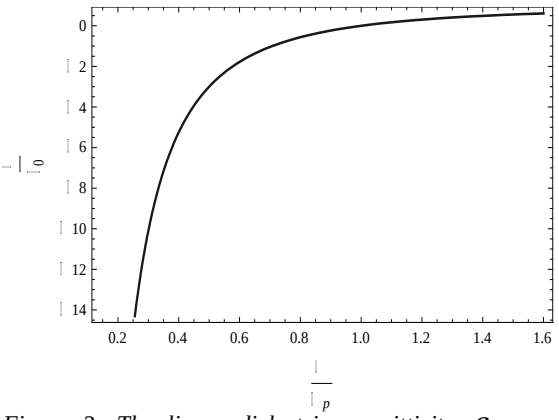

Figure 3: The linear dielectric permittivity ε as a function of frequency ω, which remains negative in the frequency band $\omega_0 < \omega < \omega_p$.

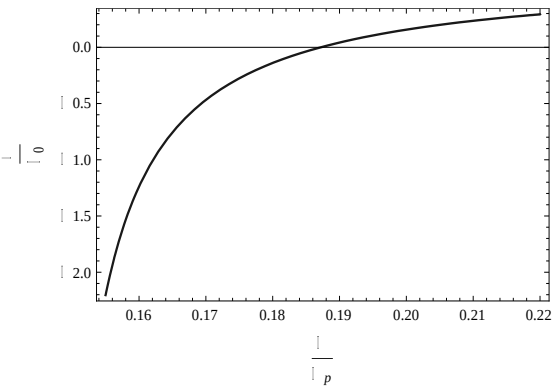

Figure 4: The linear magnetic permeability μ as a function of frequency ω, which remains negative in the frequency band $\omega_0 < \omega < \omega_M$.

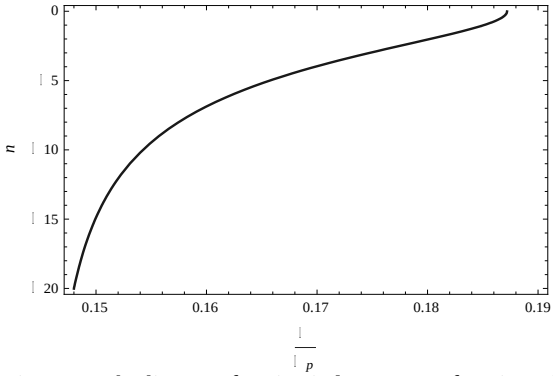

Figure 5: The linear refractive index n as a function of frequency ω, which remains negative in the frequency band $\omega_0 < \omega < \omega_M$.

II.4. Analysis of the Nonlinear Response

Now, we consider the nonlinear response on the dielectric permittivity and magnetic permeability, and on the corresponding refractive index due to applied EM fields. In this case, for weak fields we have

$$\varepsilon = \varepsilon_0\left(1-\frac{\omega_p^2}{\omega^2}+\alpha\frac{|E|^2}{E_c^2}\right), \qquad (10)$$

$$\mu = \mu_0\left(1-\frac{F\omega^2}{\omega^2-\omega_0^2}+\beta\frac{|H|^2}{E_l^2}\right). \qquad (11)$$

Considering an average value of $<\frac{|E|^2}{E_c^2}>= 0.5$ and $<\frac{|H|^2}{E_c^2}>= 0.5$, we plot ε, μ and n as functions of frequency within the frequency band, which are shown in FIG.6-8, respectively. The figures show that the frequency band for NIMs become more narrower with the applied EM fields.

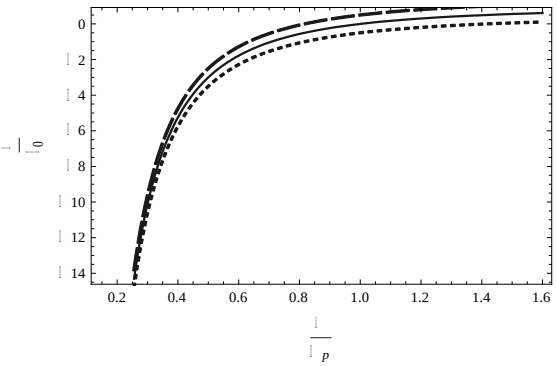

Figure 6: The nonlinear dielectric permittivity ε as a function of frequency ω under EM fields, which remains negative in the frequency band $\omega_0 < \omega < \omega_p$. Solid line (–)line for $\alpha = 0$, broken line (- - -) for $\alpha = 1$(focusing case), dotted line (...) for $\alpha = -1$(defocusing case) .

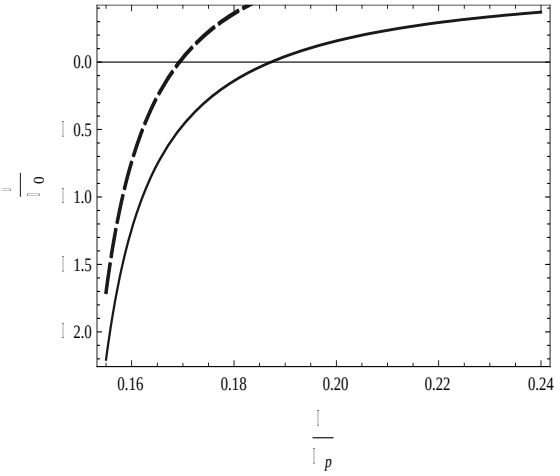

Figure 7: The nonlinear magnetic permitivity μ *as a function of frequency* ω *under EM fields, which remains negative in the frequency band* $\omega_0 < \omega < \omega_M$ *. Solid line (–)line for* $\beta = 0$ *,broken line (- - -) for* $\beta = 1$.

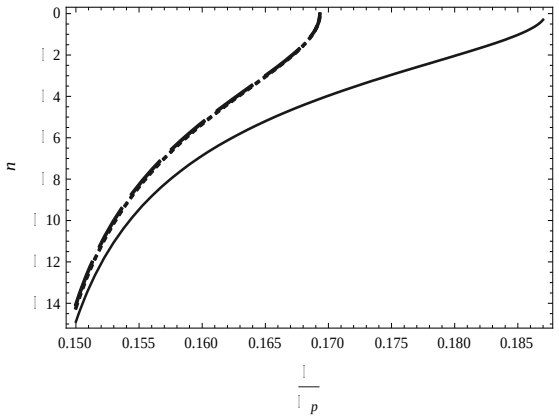

Figure 8: The nonlinear refractive index n *as a function of frequency* ω *under EM fields, which remains negative in the frequency band* $\omega_0 < \omega < \omega_M$ *. Solid line (–)line for* $\alpha = 0$ *and* $\beta = 0$*, broken line (- - -) and dotted line (....) for* $\alpha = \pm 1$ *;* $\beta = 1$.

II.5. Analysis of Magnetic Frequency ω_M

At $\omega = \omega_M$, the magnetic permeability $\mu/\mu_0 = 0$, then from Eq. (11), we get

$$1 - \frac{F\omega_M^2}{\omega_M^2 - \omega_0^2} + \beta \frac{|H|^2}{E_c^2} = 0, \qquad (12)$$

which yields

$$\omega_M^2 = \frac{\omega_0^2\left(1 + \beta \frac{|H|^2}{E_c^2}\right)}{1 + \beta \frac{|H|^2}{E_c^2} - F}. \qquad (13)$$

Introducing $\overline{H} = \frac{H}{E_c}$, we have

$$\frac{\omega_M}{\omega_0} = \left(\frac{1 + \beta|\overline{H}|^2}{1 + \beta|\overline{H}|^2 - F}\right)^{1/2}. \qquad (14)$$

For $F = .4$ and $\beta = 1$, we plot ω_M as a function of magnetic field $\overline{H}$, which is shown FIG.9. The figure shows that the magnetic frequency shifts towards the linear resonant frequency with the increase of field intensity. It indicates that the narrow frequency band is more narrowed down with the increased magnetic field.

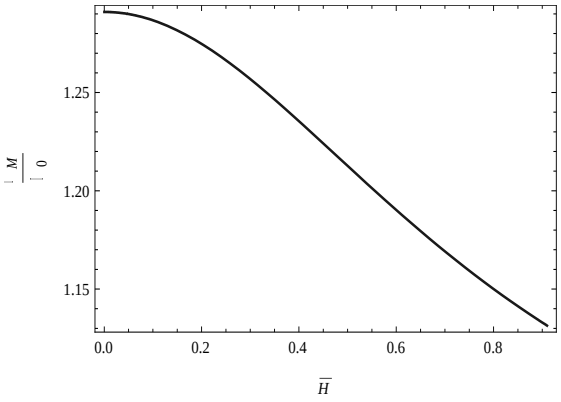

Figure 9: Magnetic frequency ω_M *as a function of magnetic field intensity* $\frac{|H|^2}{E_c^2}$ *. Here,* $\omega_M \to \omega_0$ *as* $\frac{|H|^2}{E_c^2} \to 1$·

II.6. Analysis of the Nonlinear Resonant Frequency

Following Ref. [15], the nonlinear magnetic permeability can be written as :

$$\mu\left(\omega; |H|^2\right) = 1 + \frac{F\omega^2}{\omega_{0NL}^2\left(|H|^2\right) - \omega^2 + i\Gamma\omega}, \qquad (15)$$

where, ω_{0NL} is the nonlinear resonant frequency and Γ is the loss coefficient. We also have the

expression for the nonlinear dielectric permittivity as

$$\varepsilon_D\left(|E|^2\right)=\varepsilon_{D0}+\alpha\frac{|E|^2}{E_c^2}. \qquad (16)$$

Here, ε_{D0} is the linear dielectric. Then, the relation between the macroscopic magnetic field and the dimensionless nonlinear resonant frequency can be obtained as :

$$|\overline{H}|^2=\alpha A^2\frac{\left(1-X^2\right)\left[\left(X^2-\Omega^2\right)^2+\Omega^2\gamma^2\right]}{X^6}, \quad (17)$$

where, $A^2=16\varepsilon_{D0}^3\omega_0^2h^2/c^2$, $\Omega=\omega/\omega_0$, $X=\omega_{0NL}/\omega_0$, and $\gamma=\Gamma/\omega_0$.

Near the resonant region without loss, we consider $\Omega=1,\ \gamma=0$.

Then, from Eq.(17), we find

$$\frac{\omega_{0NL}}{\omega_0}=\frac{1}{2}\left[\sqrt{\left(\frac{|\overline{H}|^2}{\alpha A^2}\right)^{2/3}+4}-\left(\frac{|\overline{H}|^2}{\alpha A^2}\right)^{1/3}\right], \quad (18)$$

which is shown graphically in FIG.8 and FIG. 9, for $\alpha=1$ (focusing nonlinearity) and $\alpha=-1$ (defocusing nonlinearity, respectively. From the available data, we find the value of the resonator parameter $A^2=2.78$.

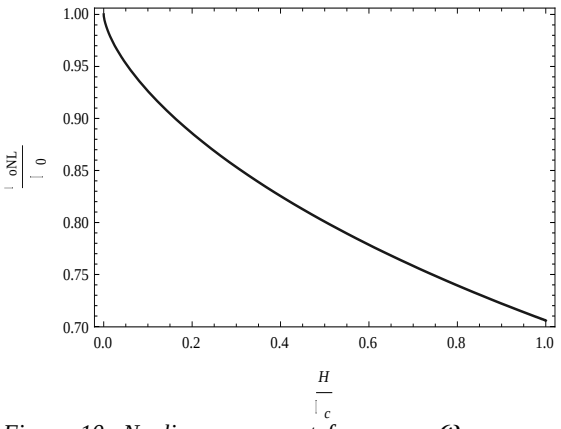

Figure 10: Nonlinear resonant frequency ω_{0NL} as a function of magnetic field intensity $|H|^2$ for $\alpha=1$ (focusing nonlinearity).

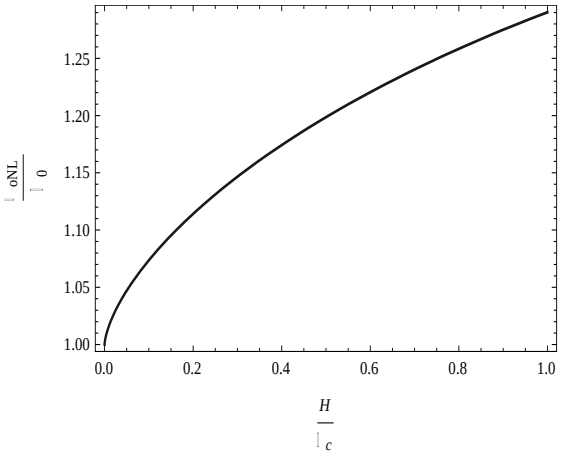

Figure 11: Nonlinear resonant frequency ω_{0NL} as a function of magnetic field intensity $|H|^2$ for $\alpha=-1$ (defocusing nonlinearity).

These figures (Fig. 10 and Fig. 11) show that the nonlinear resonant frequency ω_{0NL} goes below the linear resonant frequency ω_0 in the case of focusing ($\alpha=1$) nonlinearity and it goes up in the case of defocusing ($\alpha=-1$) nonlinearity.

III. COUPLED EVOLUTION EQUATIONS

III.1. Maxwell's Equations

We start with the Maxwell equations

$$\nabla\times\vec{E}=-\frac{\partial\vec{B}}{\partial t}, \qquad (19)$$

$$\nabla\times\vec{H}=\frac{\partial\vec{D}}{\partial t}, \qquad (20)$$

$$\nabla\cdot\vec{D}=0, \qquad (21)$$

$$\nabla\cdot\vec{B}=0, \qquad (22)$$

where, $\vec{E}$ and $\vec{H}$ are the electric and magnetic fields, respectively, $\vec{D}$ and $\vec{B}$ are the electric and magnetic flux densities which arise in response to the electric and magnetic fields inside the medium and are related to them through the constitutive relations given by $\vec{D}=(\varepsilon_L+\varepsilon_{NL})\vec{E}$, $\vec{B}=(\varepsilon_L+\varepsilon_{NL})\vec{H}$.

By using the Maxwell's systems of equations, we have the following coupled wave equations

$$\nabla^2\vec{E}-\varepsilon_L\mu_L\frac{\partial^2\vec{E}}{\partial t^2}-\mu_L\frac{\partial^2}{\partial t^2}\left(\varepsilon_{NL}\vec{E}\right)-\nabla(\nabla\cdot\vec{E})$$
$$=\frac{\partial}{\partial t}\left[\nabla\mu_{NL}\times\vec{H}\right]+\frac{\partial}{\partial t}\left(\nabla\mu_L\times\vec{E}\right)$$
$$+\frac{\partial}{\partial t}\left[\mu_{NL}\frac{\partial}{\partial t}\left\{\left(\varepsilon_L+\varepsilon_{NL}\right)\vec{H}\right\}\right], \qquad (23)$$

$$\nabla^2\vec{H}-\varepsilon_L\mu_L\frac{\partial^2\vec{H}}{\partial t^2}-\mu_L\frac{\partial^2}{\partial t^2}\left(\varepsilon_{NL}\vec{H}\right)-\nabla(\nabla\cdot\vec{H})$$
$$=\frac{\partial}{\partial t}\left[\nabla\mu_{NL}\times\vec{E}\right]+\frac{\partial}{\partial t}\left(\nabla\mu_L\times\vec{H}\right)$$
$$+\frac{\partial}{\partial t}\left[\mu_{NL}\frac{\partial}{\partial t}\left\{\left(\varepsilon_L+\varepsilon_{NL}\right)\vec{E}\right\}\right]. \qquad (24)$$

Substituting: $\varepsilon_{NL}=\varepsilon_0\alpha\,|E|^2/E_c^2$, $\mu_{NL}=\mu_0\beta\,|H|^2/E_c^2$ and taking $\nabla\equiv\hat{z}\partial/\partial z$, $E_z=H_z=0$, the above coupled equations take the following forms:

$$\frac{\partial^2\vec{E}}{\partial z^2}-\varepsilon_L\mu_L\frac{\partial^2\vec{E}}{\partial t^2}-\varepsilon_0\alpha\mu_L\frac{\partial^2}{\partial t^2}\left(\frac{|E|^2}{E_c^2}\vec{E}\right)$$
$$=\mu_0\beta\frac{\partial}{\partial t}\left[\frac{\partial}{\partial z}\left(\frac{|H|^2}{E_c^2}\right)\hat{z}\times\vec{H}\right]$$
$$+\mu_0\beta\frac{\partial}{\partial t}\left[\frac{|H|^2}{E_c^2}\left\{\varepsilon_L\frac{\partial\vec{E}}{\partial t}+\frac{\partial\varepsilon_L}{\partial t}\vec{E}\right.\right.$$
$$\left.\left.+\alpha\varepsilon_0\frac{\partial}{\partial t}\left(\frac{|E|^2}{E_c^2}\right)\vec{E}+\alpha\varepsilon_0\left(\frac{|E|^2}{E_c^2}\right)\frac{\partial\vec{E}}{\partial t}\right\}\right]$$
$$+\frac{\partial}{\partial t}\left(\frac{\partial\mu_L}{\partial z}\hat{z}\times\vec{H}\right), \qquad (25)$$

$$\frac{\partial^2\vec{H}}{\partial z^2}-\varepsilon_L\mu_L\frac{\partial^2\vec{H}}{\partial t^2}-\varepsilon_L\mu_0\beta\frac{\partial^2}{\partial t^2}\left(\frac{|H|^2}{E_c^2}\vec{H}\right)$$
$$=-\varepsilon_0\alpha\frac{\partial}{\partial t}\left[\frac{\partial}{\partial z}\left(\frac{|E|^2}{E_c^2}\right)\hat{z}\times\vec{E}\right]$$
$$+\varepsilon_0\alpha\frac{\partial}{\partial t}\left[\frac{|E|^2}{E_c^2}\left\{\mu_L\frac{\partial\vec{H}}{\partial t}+\frac{\partial\mu_L}{\partial t}\vec{H}\right.\right.$$
$$\left.\left.+\mu_0\beta\frac{\partial}{\partial t}\left(\frac{|H|^2}{E_c^2}\right)\vec{H}+\mu_0\beta\left(\frac{|H|^2}{E_c^2}\right)\frac{\partial\vec{H}}{\partial t}\right\}\right]$$
$$+\frac{\partial}{\partial t}\left(\frac{\partial\varepsilon_L}{\partial z}\hat{z}\times\vec{E}\right). \qquad (26)$$

Now, considering that the laser radiation is circularly polarized, i. e. $\vec{E}=\{E_x,E_y,0\}$, $\vec{H}=\{H_x,H_y,0\}$ and introducing the complex fields: $\tilde{E}=E_x\pm iE_y$, $\tilde{H}=H_x\pm iH_y$, from Eqns. (25) and (26), we find the following coupled equations for the complex fields:

$$\frac{\partial^2\tilde{E}}{\partial z^2}-\varepsilon_L\mu_L\frac{\partial^2\tilde{E}}{\partial t^2}-\varepsilon_0\alpha\mu_L\frac{\partial^2}{\partial t^2}\left(\frac{|E|^2}{E_c^2}\tilde{E}\right)$$
$$=\pm i\mu_0\beta\frac{\partial}{\partial t}\left[\frac{\partial}{\partial z}\left(\frac{|H|^2}{E_c^2}\right)\tilde{H}\right]$$
$$+\mu_0\beta\frac{\partial}{\partial t}\left[\frac{|H|^2}{E_c^2}\left\{\varepsilon_L\frac{\partial\tilde{E}}{\partial t}+\frac{\partial\varepsilon_L}{\partial t}\tilde{E}\right.\right.$$
$$\left.\left.+\alpha\varepsilon_0\frac{\partial}{\partial t}\left(\frac{|E|^2}{E_c^2}\right)\tilde{E}+\alpha\varepsilon_0\left(\frac{|E|^2}{E_c^2}\right)\frac{\partial\tilde{E}}{\partial t}\right\}\right]$$
$$\pm i\frac{\partial}{\partial t}\left(\frac{\partial\mu_L}{\partial z}\tilde{H}\right), \qquad (27)$$

$$\frac{\partial^2\tilde{H}}{\partial z^2}-\varepsilon_L\mu_L\frac{\partial^2\tilde{H}}{\partial t^2}-\varepsilon_L\mu_0\beta\frac{\partial^2}{\partial t^2}\left(\frac{|H|^2}{E_c^2}\tilde{H}\right)$$
$$=\mp i\varepsilon_0\alpha\frac{\partial}{\partial t}\left[\frac{\partial}{\partial z}\left(\frac{|E|^2}{E_c^2}\right)\tilde{E}\right]$$
$$+\varepsilon_0\alpha\frac{\partial}{\partial t}\left[\frac{|E|^2}{E_c^2}\left\{\mu_L\frac{\partial\tilde{H}}{\partial t}+\frac{\partial\mu_L}{\partial t}\tilde{H}\right.\right.$$

$$+\mu_0\beta\frac{\partial}{\partial t}\left(\frac{|H|^2}{E_c^2}\right)\tilde{H}+\mu_0\beta\left(\frac{|H|^2}{E_c^2}\right)\frac{\partial\tilde{H}}{\partial t}\Bigg\}\Bigg]$$

$$\pm i\frac{\partial}{\partial t}\left(\frac{\partial\varepsilon_L}{\partial z}\tilde{E}\right), \qquad (28)$$

which we study below for the high frequency and the low frequency responses to the fields.

III.2. High Frequency Response and Nonlinear Dispersion Relation

Taking $\tilde{E}=\mathsf{E}(z,t)\exp[i(kz-\omega t)]$ and $\tilde{H}=\mathsf{H}(z,t)\exp[i(kz-\omega t)]$ with $(1/|\mathsf{E}|)\partial|\mathsf{E}|/\partial t<<\omega$, $(1/|\mathsf{E}|)\partial|\mathsf{E}|/\partial z<<k$, and considering $\frac{\partial\varepsilon_L}{\partial t}=0,\ \frac{\partial\mu_L}{\partial t}=0,\frac{\partial\varepsilon_L}{\partial z}=0,$ $\frac{\partial\mu_L}{\partial z}=0,$ from Eqn. (27) or Eqn.(28) we find the the following field dependent nonlinear dispersion relation:

$$\omega=k\Bigg[\varepsilon_L\mu_L+\varepsilon_0\mu_L\alpha\left(\frac{|E|^2}{E_c^2}\right)+\mu_0\varepsilon_L\beta\left(\frac{|H|^2}{E_c^2}\right)$$

$$+\varepsilon_0\mu_0\alpha\beta\left(\frac{|E|^2}{E_c^2}\right)\left(\frac{|H|^2}{E_c^2}\right)\Bigg]^{-1/2}. \qquad (29)$$

Now, introducing the dimensionless parmeters:

$$\bar{\omega}=\frac{\omega}{\omega_p},\ \bar{\omega}_0=\frac{\omega_0}{\omega_p}\ \text{with}\ \frac{1}{\sqrt{\varepsilon_0\mu_0}}=c,$$

and writing ε_L and μ_L as

$$\varepsilon_L=\varepsilon_0\left(1-\frac{1}{\bar{\omega}^2}\right)\equiv\varepsilon_0\bar{\varepsilon}(\bar{\omega}), \qquad (30)$$

$$\mu_L=\mu_0\left(1-\frac{F\bar{\omega}^2}{\bar{\omega}^2-\bar{\omega}_0^2}\right)\equiv\mu_0\bar{\mu}(\bar{\omega}), \qquad (31)$$

where ,

$$\bar{\varepsilon}(\bar{\omega})=1-\frac{1}{\bar{\omega}^2} \qquad (32)$$

$$\bar{\mu}(\bar{\omega})=1-\frac{F\bar{\omega}^2}{\bar{\omega}^2-\bar{\omega}_0^2} \qquad (33)$$

the above dispersion relation (Eq.(29)) can also be written in the following form:

$$\omega=kc\Bigg[\bar{\varepsilon}(\bar{\omega})\bar{\mu}(\bar{\omega})+\bar{\mu}(\bar{\omega})\alpha\left(\frac{|\mathsf{E}|^2}{E_c^2}\right)+\bar{\varepsilon}(\bar{\omega})\beta\left(\frac{|\mathsf{H}|^2}{E_c^2}\right)$$

$$+\alpha\beta\left(\frac{|\mathsf{E}|^2}{E_c^2}\right)\left(\frac{|\mathsf{H}|^2}{E_c^2}\right)\Bigg]^{-1/2}. \qquad (34)$$

The group velocity $v_g=\partial\omega/\partial k$ is found to be

$$v_g=c\Bigg[\bar{\varepsilon}(\bar{\omega})\bar{\mu}(\bar{\omega})+\alpha\bar{\mu}(\bar{\omega})\left(\frac{|\mathsf{E}|^2}{E_c^2}\right)+\beta\bar{\varepsilon}(\bar{\omega})\left(\frac{|\mathsf{H}|^2}{E_c^2}\right)$$

$$+\alpha\beta\left(\frac{|\mathsf{E}|^2}{E_c^2}\right)\left(\frac{|\mathsf{H}|^2}{E_c^2}\right)\Bigg]^{-1/2}. \qquad (35)$$

We plot the group velocity v_g as a function of the frequency ω in the frequency band $\omega_0<\omega<\omega_M$ for both the linear and nonlinear cases, which are shown in FIG.12. The figure shows that the frequency band for the wave propagation is more narrowed down (ω_M decreases) in the nonlinear case with the increase of field intensities.

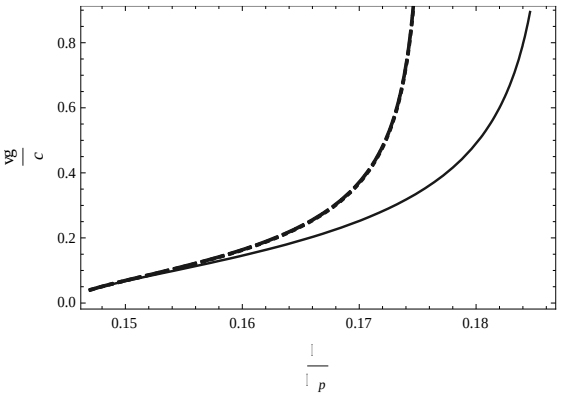

Figure 12: Group velocity v_g as a function of frequency ω in the frequency band $\omega_0<\omega<\omega_M$. Solid line (—-) is the linear case, dash and dot lines(- - -) for nonlinear case for $\beta=1,\frac{|\mathsf{E}|^2}{E_c^2}=.5,\frac{|\mathsf{H}|^2}{E_c^2}=.5$ and $\alpha=\pm1$, respectively.

III.3. Low Frequency Response: Coupled NLS Equations

Normalizing the field variables E and H by E_c and introducing dimensionless space-time coordinates: $Z = z/\lambda_p$, and $T = t/t_p$, where λ_p is the pulse length, and t_p is the pulse time with $\lambda_p = ct_p$, the coupled equations, Eqs. (27) and (28) in dimensionless forms are:

$$\frac{\partial^2 \tilde{E}}{\partial Z^2} - \bar{\varepsilon}(\bar{\omega})\bar{\mu}(\bar{\omega})\frac{\partial^2 \tilde{E}}{\partial T^2}$$

$$- \overline{\alpha\mu}(\bar{\omega})\frac{\partial^2 |\tilde{E}|^2}{\partial T^2}\tilde{E} - \overline{\alpha\mu}(\bar{\omega})|\tilde{E}|^2 \frac{\partial^2 \tilde{E}}{\partial T^2}$$

$$= \pm i\beta\sqrt{\frac{\mu_0}{\varepsilon_0}}\left[\frac{\partial^2 |\tilde{H}|^2}{\partial T \partial Z}\tilde{H} + \frac{\partial |\tilde{H}|^2}{\partial Z}\frac{\partial \tilde{H}}{\partial T}\right]$$

$$+ \alpha\beta\left[\frac{\partial |\tilde{H}|^2}{\partial T}\frac{\partial |\tilde{E}|^2}{\partial T}\tilde{E} + |\tilde{H}|^2 \frac{\partial^2 |\tilde{E}|^2}{\partial T^2}\tilde{E}\right.$$

$$\left. + |\tilde{H}|^2 \frac{\partial |\tilde{E}|^2}{\partial T}\frac{\partial \tilde{E}}{\partial T}\right]$$

$$+ \beta\bar{\varepsilon}(\bar{\omega})\left[\frac{\partial |\tilde{H}|^2}{\partial T}\frac{\partial \tilde{E}}{\partial T} + |\tilde{H}|^2 \frac{\partial^2 \tilde{E}}{\partial T^2}\right]$$

$$+ \beta\overline{\frac{\partial \bar{\varepsilon}(\bar{\omega})}{\partial T}}\left[\frac{\partial |\tilde{H}|^2}{\partial T}\tilde{E} + 2|\tilde{H}|^2 \frac{\partial \tilde{E}}{\partial T}\right]$$

$$+ \beta\frac{\partial^2 \bar{\varepsilon}(\bar{\omega})}{\partial T^2}|\tilde{H}|^2 \tilde{E} +$$

$$+ \alpha\beta\left[\frac{\partial |\tilde{H}|^2}{\partial T}\frac{\partial \tilde{E}}{\partial T}|\tilde{E}|^2 + |\tilde{H}|^2 \frac{\partial |\tilde{E}|^2}{\partial T}\frac{\partial \tilde{E}}{\partial T}\right.$$

$$\left. + |\tilde{H}|^2 |\tilde{E}|^2 \frac{\partial^2 \tilde{E}}{\partial T^2}\right]$$

$$\pm i\sqrt{\frac{\mu_0}{\varepsilon_0}}\left[\frac{\partial^2 \bar{\mu}(\bar{\omega})}{\partial T \partial Z}\tilde{H} + \frac{\bar{\mu}(\bar{\omega})}{\partial Z}\frac{\partial \tilde{H}}{\partial T}\right], \quad (36)$$

and

$$\frac{\partial^2 \tilde{H}}{\partial Z^2} - \bar{\varepsilon}(\bar{\omega})\bar{\mu}(\bar{\omega})\frac{\partial^2 \tilde{H}}{\partial T^2}$$

$$- \bar{\varepsilon}(\bar{\omega})\beta\frac{\partial^2 |\tilde{H}|^2}{\partial T^2}\tilde{H} - \bar{\varepsilon}(\bar{\omega})\beta|\tilde{H}|^2 \frac{\partial^2 \tilde{H}}{\partial T^2}$$

$$= \mp i\alpha\sqrt{\frac{\varepsilon_0}{\mu_0}}\left[\frac{\partial^2 |\tilde{E}|^2}{\partial T \partial Z}E_x + \frac{\partial |\tilde{E}|^2}{\partial Z}\frac{\partial \tilde{E}}{\partial T}\right]$$

$$+ \alpha\beta\left[\frac{\partial |\tilde{E}|^2}{\partial T}\frac{\partial |\tilde{H}|^2}{\partial T}\tilde{H} + |\tilde{E}|^2 \frac{\partial^2 |\tilde{H}|^2}{\partial T^2}\tilde{H}\right.$$

$$\left. + |\tilde{E}|^2 \frac{\partial |\tilde{H}|^2}{\partial T}\frac{\partial \tilde{H}}{\partial T}\right]$$

$$+ \alpha\bar{\mu}(\bar{\omega})\left[\frac{\partial |\tilde{E}|^2}{\partial T}\frac{\partial \tilde{H}}{\partial T} + |\tilde{E}|^2 \frac{\partial^2 \tilde{H}}{\partial T^2}\right]$$

$$+ \alpha\beta\left[\frac{\partial |\tilde{E}|^2}{\partial T}\frac{\partial \tilde{H}}{\partial T}|\tilde{H}|^2 + |\tilde{E}|^2 \frac{\partial |\tilde{H}|^2}{\partial T}\frac{\partial \tilde{H}}{\partial T}\right.$$

$$\left. + |\tilde{E}|^2 |\tilde{H}|^2 \frac{\partial^2 \tilde{H}}{\partial T^2}\right]$$

$$\pm i\sqrt{\frac{\varepsilon_0}{\mu_0}}\left[\frac{\partial^2 \bar{\alpha}(\bar{\omega})}{\partial T \partial Z}\tilde{E} + \frac{\bar{\alpha}(\bar{\omega})}{\partial Z}\frac{\partial \tilde{E}}{\partial T}\right]. \quad (37)$$

Now, we consider the following Lorentz invariant stretched coordinates [16]: $\xi = \delta\gamma(Z - v_g T)$ and $\tau = \delta^2\gamma(T - v_g Z)$, where $\gamma \equiv (1 - v_g^2)^{-1/2}$, $\delta < 1, v_g \equiv v_g/c$, and we expand the quantities $\tilde{E}$ and $\tilde{H}$ as:

$$\tilde{E} = \delta^2 \mathsf{E}_0 + \sum_{l=1}^{\infty}\delta^l\left(\mathsf{E}_l e^{il(kZ-\omega T)} + \mathsf{E}_l^* e^{-il(kZ-\omega T)}\right), \quad (38)$$

$$\tilde{H} = \delta^2 \mathsf{H}_0 + \sum_{l=1}^{\infty}\delta^l\left(\mathsf{H}_l e^{il(kZ-\omega T)} + \mathsf{H}_l^* e^{-il(kZ-\omega T)}\right). \quad (39)$$

Here,

$$(\mathsf{E}_0, \mathsf{H}_0, \mathsf{E}_l, \mathsf{H}_l) \equiv A^{(1)} + \delta A^{(2)} + \delta^2 A^{(3)} + \ldots$$

are functions of stretched coordinates (ξ, τ).

Then in the order $0(\delta)$, we find $\omega = k/\sqrt{\bar{\varepsilon}\bar{\mu}}$, and in the order $0(\delta^2)$, we find $v_g = 1/\sqrt{\bar{\varepsilon}\bar{\mu}}$ approving the compatibility condition. Thus, following the standard technique [17] in the order $0(\delta^3)$, we arrive at the following coupled NLS equations:

$$i\frac{\partial a}{\partial \tau}+P\frac{\partial^2 a}{\partial \xi^2}+Q_a\,|\,a\,|^2\,a+Q_b\,|\,b\,|^2\,a=0, \quad (40)$$

$$i\frac{\partial b}{\partial \tau}+P\frac{\partial^2 b}{\partial \xi^2}+Q_b\,|\,b\,|^2\,b+Q_a\,|\,a\,|^2\,b=0, \quad (41)$$

where $a\equiv \mathsf{E}_1^{(1)}$, $b\equiv \mathsf{H}_1^{(1)}$ and P, Q_a, Q_b are given by the expressions

$$P=\frac{\gamma\left(1-\bar{\varepsilon}\,\bar{\mu}v_g^2\right)}{2\omega\left(\bar{\varepsilon}\,\bar{\mu}-kv_g/\omega\right)}, \quad (42)$$

$$Q_a=\frac{\alpha\omega\bar{\mu}}{2\gamma\left(\bar{\varepsilon}\,\bar{\mu}-kv_g/\omega\right)}, \quad (43)$$

and

$$Q_b=\frac{\beta\omega\bar{\varepsilon}}{2\gamma\left(\bar{\varepsilon}\,\bar{\mu}-kv_g/\omega\right)}. \quad (44)$$

Here, P is the dispersion coefficient, Q_a and Q_b are the nonlinear coefficients, the nature of which on the frequency ω in the frequency band $\omega_0<\omega<\omega_M$, we study below.

III.4. Analysis of P, Q_a, and Q_b

Taking the parameters $F=0.4$, $\bar{\omega}_0=0.145$, $<|a|^2>=0.5$, $<|b|^2>=0.5$, $\alpha=\pm 1$, and $\beta=1$, the plots of P, Q_a, Q_b, and $Q=Q_a+Q_b$ are depicted in FIGs. 13-17, respectively.

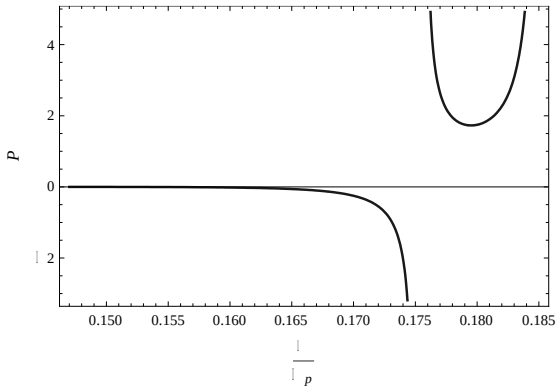

Figure 13: Dispersion coefficient P as a function of frequency ω in the frequency band $\omega_0<\omega<\omega_M$. P changes its sign from negative to positive at a critical frequency $\bar{\omega}_{cr}\approx 0.1742$.

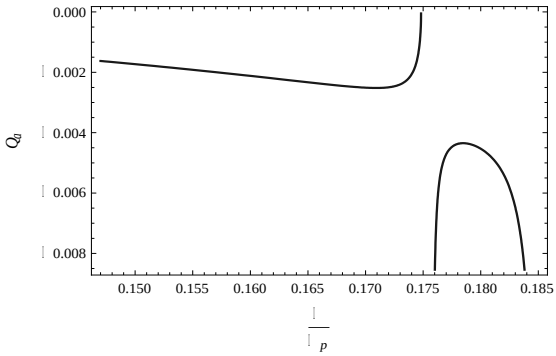

Figure 14: The nonlinear coefficient Q_a as a function of frequency ω in the frequency band $\omega_0<\omega<\omega_M$. Q_a is always negative but changes its value abruptly at a critical frequency $\bar{\omega}_{cr}\approx 0.1742$ for $\alpha=1$ (focusing nonlinearity)

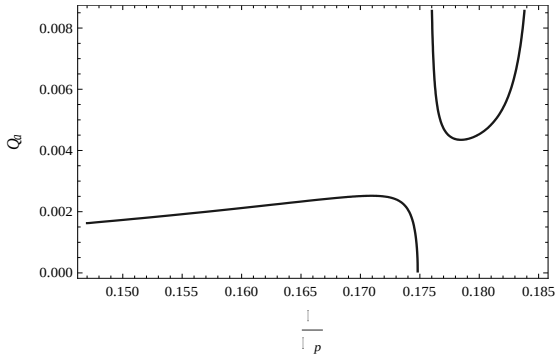

Figure 15: The nonlinear coefficient Q_a as a function of frequency ω in the frequency band $\omega_0<\omega<\omega_M$. Q_a is always negative but changes its value abruptly at a critical frequency $\bar{\omega}_{cr}\approx 0.1742$ for $\alpha=-1$ (defocusing nonlinearity)

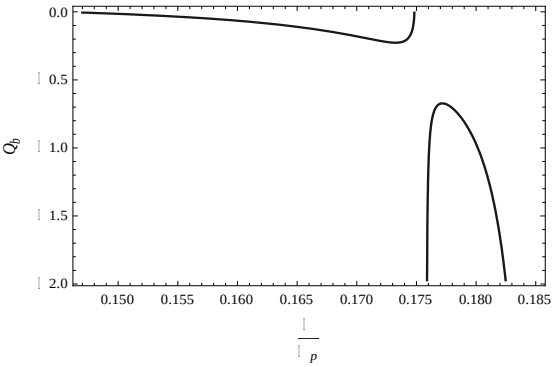

Figure 16: The nonlinear coefficient Q_b as a function of frequency ω in the frequency band $\omega_0<\omega<\omega_M$. Q_b is always negative but changes its value abruptly at a critical frequency $\bar{\omega}_{cr}\approx 0.1742$.

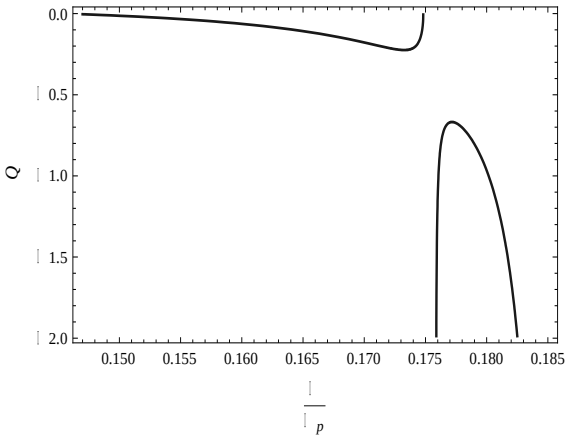

Figure 17: The nonlinear coefficient Q *as a function of frequency* ω *in the frequency band* $\omega_0 < \omega < \omega_M$. Q *is always negative but changes its value abruptly at a critical frequency* $\overline{\omega}_{cr} \approx 0.1742$.

We see from the Figs. 13-17 that P changes its sign from negative to positive , Q_a is negative for focusing ($\alpha = 1$) nonlinearity while it is positive for defocusing($\alpha = -1$) nonlinearity , Q_b an Q are always negative but change their values abruptly at a certain critical frequency $\overline{\omega}_{cr}$, which is defined by the condition at $v_g/c = 1$, and it is determined from the Eq.(35) as

$$\overline{\omega}_{cr} = \sqrt{\frac{-\hat{b} - \sqrt{\hat{b}^2 - 2\hat{a}\hat{c}}}{2\hat{a}}}, \qquad (45)$$

where,

$$\hat{a} = -F + \beta Y^2 + (1-F)\alpha X^2 + \alpha\beta X^2 Y^2,$$
$$\hat{b} = -(1-F) - \omega_0^2(\alpha X^2 + \beta Y^2 + \alpha\beta X^2 Y^2) - \beta Y^2,$$
$$\hat{c} = \omega_0^2(1+\beta Y^2). \quad (37)$$

Here, $X = \frac{|\mathsf{E}|}{E_c}$ and $Y = \frac{|\mathsf{H}|}{E_c}$.

For $\beta = 1, X = 0.5, Y = 0.5, \overline{\omega}_0 = 0.145, F = 0.4$, we find $\overline{\omega}_{cr} = 0.174822$ for $\alpha = 1$, and $\overline{\omega}_{cr} = 0.174837$ for $\alpha = -1$, respectively. Considering the same intensities of electric and magnetic fields: $X^2 = Y^2$, we plot the graph of $\overline{\omega}_{cr}$ as a function of field $X = Y$, which is shown in FIG.18. The figure shows that the critical frequency $\overline{\omega}_{cr}$ goes to the linear resonant frequency $\overline{\omega}_0$ with the increase of intensities of the wave fields.

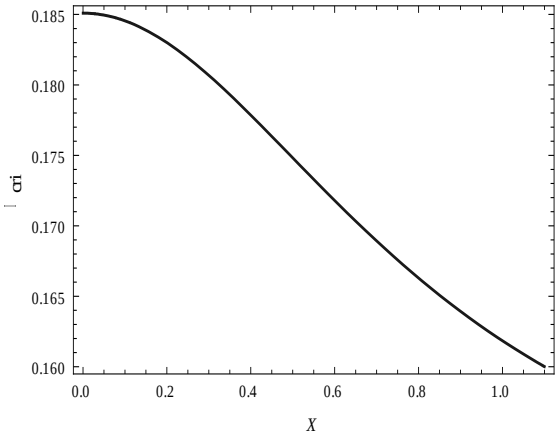

Figure 18: $\overline{\omega}_{cr}$ *as a function of applied field* $X = Y$. *Note that* $\overline{\omega}_{cr} \to \overline{\omega}_0$ *as* $X \to 1$.

III.5. Solution of the NLSE

From the symmetric nature of Eqs. (40) and (41) and considering the same intensities of the electric and magnetic fields of the wave, we can take $|a|^2 = |b|^2$ [18]. In this situation, we obtain from either of Eq. (40) or Eq. (41)

$$i\frac{\partial a}{\partial \tau} + P\frac{\partial^2 a}{\partial \xi^2} + Q|a|^2 a = 0, \qquad (46)$$

where, $Q = Q_a + Q_b$. In the present situation, it is seen that, P can be positive as well as negative for different range of the values of the frequency $\overline{\omega}$, whereas Q is always negative. Thus, for obtaining solution of the above Eq. (46), we may have two cases: Case I: $\overline{\omega}_0 < \overline{\omega} < \overline{\omega}_{cr}$; where $P < 0$, $Q < 0$, and $PQ > 0$ and Case II: $\overline{\omega}_{cr} < \overline{\omega} < \overline{\omega}_M$; where $P > 0$, $Q < 0$, and $PQ < 0$. For the case I, we take a new variable η such that $\eta = \xi - V\tau$ and assume $a(\xi,\tau) = u(\eta)\exp[i(K\xi + \Omega\tau)]$, where V is a constant, then from Eq. (46) we find:

$$(2PK - V)\frac{du}{d\eta} = 0, \quad (47)$$

$$P\frac{d^2u}{d\eta^2} - \left(PK^2 + \Omega\right)u + Qu^3 = 0, \quad (48)$$

which gives $K = V/2P$ and yields an integral of motion

$$\left(\frac{du}{d\eta}\right)^2 - \left(\frac{PK^2 + \Omega}{P}\right)u^2 + \frac{Q}{2P}u^4 = const. \quad (49)$$

For a localized solution, we consider $u, du/\eta \to 0$ as $\eta \to \pm\infty$, and so, we put $const. = 0$. At the maximum value of $u = u_0$, $du/d\eta = 0$, which defines $\Omega = Qu_0^2/2 - V^2/4P$.

Thus, we arrive at the following solution of Eq.(49)

$$u(\eta) = a_0\, sech\left(a_0\sqrt{\frac{Q}{2P}}\eta\right), \quad (50)$$

where a_0 is a constant. Going back to the (ξ, τ) coordinates, we have the solution of Eq. (46) as

$$a(\xi,\tau) = a_0\, sech\left[a_0\sqrt{\frac{Q}{2P}}(\xi - V\tau)\right] \times e^{i\left\{\frac{V}{2P}\xi + \frac{1}{2}\left(Qa_0^2 - \frac{V^2}{2P}\right)\tau\right\}}, \quad (51)$$

which is a bump type solution, known as the bright soliton, and the wave amplitude may be modulationally unstable. Similarly, the solution for Case II ($PQ < 0$) is [19]:

$$a(\xi,\tau) = \left[a_0\, tanh\left\{a_0\sqrt{\left|\frac{Q}{2P}\right|}(\xi - V\tau)\right\} - i\sqrt{\left|\frac{2P}{Q}\right|}\left(D - \frac{V}{2P}\right)\right] \times e^{i\left\{D\xi + \left(u_0^2 Q - 3PD^2 + 2DV - \frac{V^2}{2P}\right)\tau\right\}}, \quad (52)$$

Here, a_0, V and D are arbitrary constants. They define gray solitons . For $V = 2PD$, it is a kink type dark soliton. Below, we investigate the modulational instabilities of these solitons.

III.6. Modulations instabilities of optical solitons

Coherent dispersion: Hasegawa Formalism

In order to investigate the modulational instability of optical solitons, we follow Hasegwawa formalism [20,21]. Considering the modulation of a constant amplitude coherent phase dispersion, we introduce a phase shift $a \to aExp(iQ\,|\,a_0\,|^2\,\tau)$, where a_0 is the constant equilibrium amplitude of the field. Then, Eq.(46) can be written as:

$$i\frac{\partial a}{\partial \tau} + P\frac{\partial^2 a}{\partial \xi^2} + Q(|\,a\,|^2 - |\,a_0\,|^2)a = 0. \quad (53)$$

In a polar representation, we write $a = \rho Exp(i\psi)$, where $\rho = \rho(\xi,\tau)$ and $\psi = \psi(\xi,\tau)$ .This means that $\rho = |\,a\,|$ with an equilibrium value $\rho_0 = |\,a_0\,|$. Equation(53) has the obvious solution $\rho = \rho_0, \psi = 0$.

Let $\rho = \rho_0 + \rho_1$, where $|\,\rho_1\,| << \rho_0$ and $\psi = \psi_1$. Then by linearizing Eq.(53) from the imaginary and real parts , we obtain

$$\frac{\partial \rho_1}{\partial \tau} + P\rho_0\frac{\partial^2 \psi_1}{\partial \xi^2} = 0. \quad (54)$$

$$\frac{\partial \psi_1}{\partial \tau} - \frac{P}{\rho_0}\frac{\partial^2 \rho_1}{\partial \xi^2} - 2Q\rho_0\rho_1 = 0. \quad (55)$$

which yield

$$\frac{\partial^2 \rho_1}{\partial \tau^2} + P^2\frac{\partial^4 \rho_1}{\partial \xi^4} + 2QP\rho_0^2\rho_1 = 0. \quad (56)$$

Considering, $\rho_1 = \bar{\rho}_1 Exp(iK\xi - \Omega\tau)$,we readily obtain from Eq.56), the nonlinear dispersion relation

$$\Omega^2 = PK^2(PK^2 - 2Q\rho_0^2) = P^2K^2(K^2 - \frac{2Q}{P}\rho_0^2) = (PK^2 - Q\rho_0^2)^2 - Q^2\rho_0^4. \quad (57)$$

We see from Eq.(57) that if $Q/P > 0$, Ω^2 becomes negative for values of K below $K_{cr} = \sqrt{\frac{2Q}{P}}\,|\rho_0|$, so that there is a purely growing mode and the wave is modulationally unstable. The growth rate $\sigma = Im(\Omega)$ attains a maximum $\sigma_{max} = Q\,|\rho_0|^2$ for $K = \sqrt{\frac{Q}{P}}\,|\rho_0|$. Therefore, in dimensionless variables: $\bar{\sigma} = \sigma/\sigma_{max}$, $\bar{K} = K/K_{cr}$:

$$\bar{\sigma} = \sqrt{1-(2\bar{K}^2-1)^2}. \qquad (58)$$

FIG.19 shows the variation of the growth rate $\bar{\sigma}$ as a function of the wave number $\bar{K}$. On the other hand, for $Q/P < 0$, the wave is modulationally stable.

It is to be noted that for a fixed amplitude ρ_0, the critical frequency K_{cr} is a function of frequencies $\bar{\omega}$ in the frequency band, which is shown in FIG. 20.

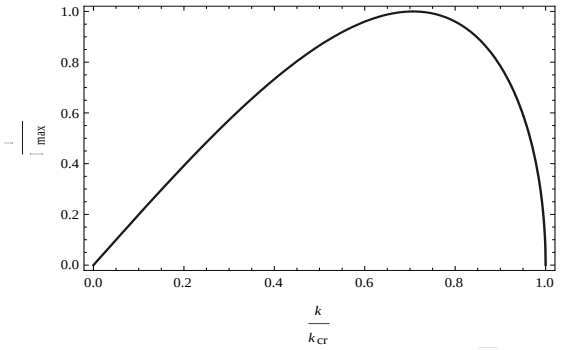

Figure 19: The growth rate $\bar{\sigma}$ as a function of K.

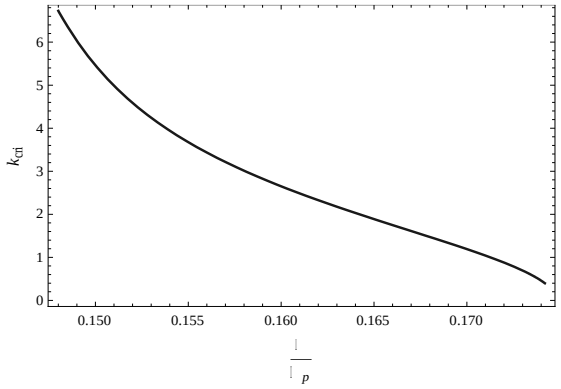

Figure 20: K_{cr} as a function frequency $\bar{\omega}$ in the frequency band for $\rho_0 = 1$.

A. Fast Mode: Bright Soliton

We see from above, the fast mode has $PQ > 0$, and thus modulationally unstable. Possible final state can lead to the formation of bright soliton, i.e. a localized envelope modulating a carrier wave in the form $a = \rho Exp(i\psi)$, where

$$\rho = \frac{1}{L}\sqrt{\frac{2P}{Q}}\,sech\left(\frac{\xi - V\tau}{L}\right). \qquad (59)$$

and

$$\psi = \frac{1}{2P}\left[V\xi + \left(\frac{\sqrt{2}P}{L} - \frac{V^2}{2}\right)\tau\right] + \psi_0. \qquad (60)$$

where, V is the envelope speed, L is the pulse spatial width at $\tau = 0$ and ψ_0 is an arbitrary phase. The maximum amplitude ρ_0 is inversely proportional to the width L, i.e. $\rho_0 L = \sqrt{2P/Q}$. We do an analysis of pulse width L on the frequencies within the band, which is shown in Fig. 21. It shows that the width is narrower at the resonant frequency while it becomes wider at higher frequencies.

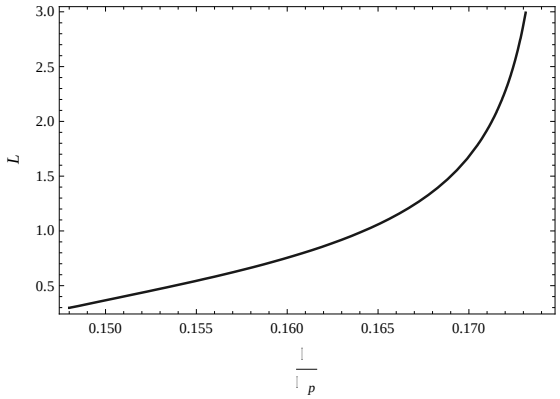

Figure 21: Pulse width L as a function frequency $\bar{\omega}$ within the frequency band for $\rho_0 = 1$.

At a fixed time $\tau = 0$, we have shown modulational envelopes of the carrieer wave and the corresponding bright solitons at different fixed frequencies within the frequency band in FIGs. 22-23 for $L = .5$ and FIGs. 24-25 for $L = 2$, respectively.

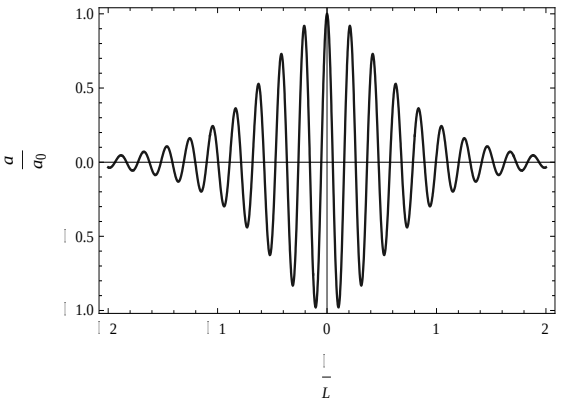

Figure 22: Modulational envelope of fast mode for $L = .5$ *corresponding to* $\omega/\omega_p = .155, V/2P = 30$ *at* $\tau = 0$.

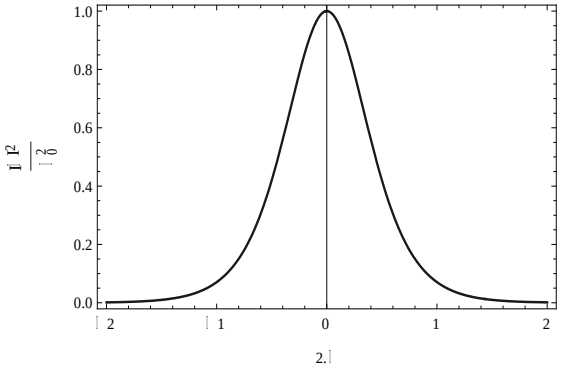

Figure 23: Bright soliton for $L = .5$ *corresponding to* $\omega/\omega_p = .155$, *at* $\tau = 0$.

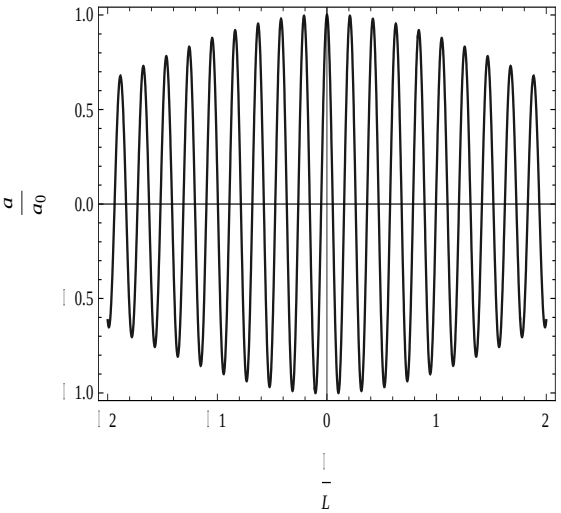

Figure 24: Modulational envelope of fast mode for $L = 2$, *corresponding to* $\omega/\omega_p = .17$, $V/2P = 30$ *at* $\tau = 0$.

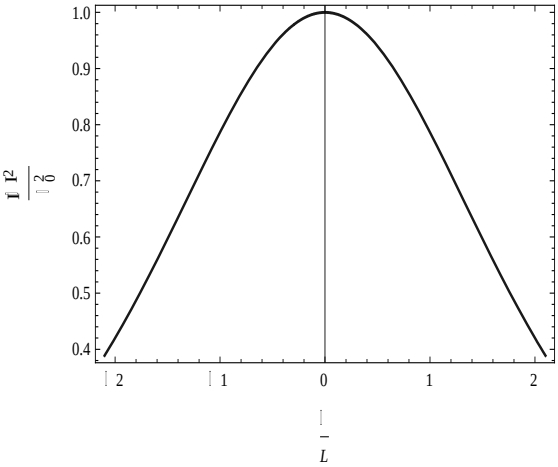

Figure 25: Bright soliton for $L = 2$ *corresponding to* $\omega/\omega_p = .17$, *at* $\tau = 0$.

B. The slow mode: Dark Soliton

The slow mode is modulationally stable since $PQ < 0$. It produces dark and gray solitons[22]. The dark has

$$\rho = \frac{1}{L}\sqrt{\frac{2P}{Q}}\tanh\left(\frac{\xi - V\tau}{L}\right). \tag{61}$$

and

$$\psi = \frac{1}{2P}\left(V\xi - \frac{V^2}{2}\tau\right) + \psi_0, \tag{62}$$

while the gray has

$$\rho = \sqrt{|\frac{2P}{Q}|}\,\frac{1}{Ld}\sqrt{1 - d^2\,\mathrm{sech}^2\left(\frac{\xi - V\tau}{L}\right)}. \tag{63}$$

and

$$\psi = \frac{1}{2P}\left(V_0\xi - \frac{V_0^2}{2}\tau\right) + s\cdot\arcsin\frac{d\cdot\tanh\left(\frac{\xi - V\tau}{L}\right)}{\sqrt{1 - d^2\,\mathrm{sech}^2\left(\frac{\xi - V\tau}{L}\right)}} + \psi_0. \tag{64}$$

Here, the parameter d, lying in the range $0 < d < 1$, regulates the modulation depth, $s = \pm 1$, and $V_0 = V + s(2P/Ld)\sqrt{1-d^2}$. Note that for $d = 1$, one recovers the dark soliton. The finite equilibrium amplitude ρ_0 is now inversely proportional to both the width L and the parameter d, i.e. $\rho_0 Ld = \sqrt{2|P/Q|}$. The minimum amplitude is given by $\rho_{min} = \rho_0\sqrt{1-d^2}$, which is zero in the dark case. FIGs 26-29 show the modulational envelopes of the carrieer wave and the corresponding dark solitons at different frequencies within the frequency band at a fixed time $\tau = 0$ for $L = .5$ and $L = 2$, respectively.

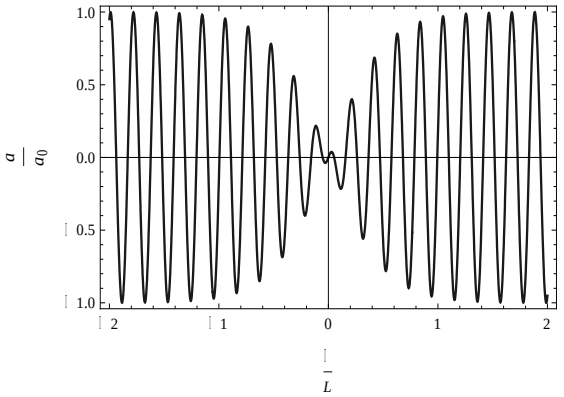

Figure 26: Modulational envelope of slow mode for $L = .5$ *corresponding* $\omega/\omega_p = .155$, $V/2P = 30$ *at* $\tau = 0$.

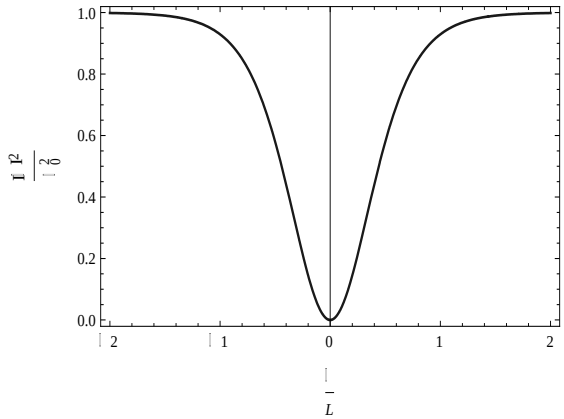

Figure 27: Dark soliton for $L = .5$ *corresponding to* $\omega/\omega_p = .155$, *at* $\tau = 0$.

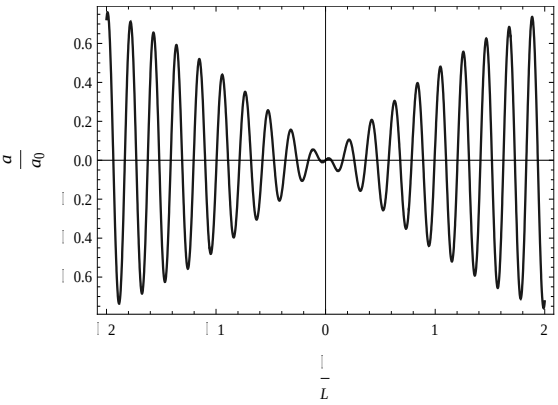

Figure 28: Modulational envelope for slow mode $L = 2$, *corresponding to* $\omega/\omega_p = .17$, $V/2P = 30$ *at* $\tau = 0$.

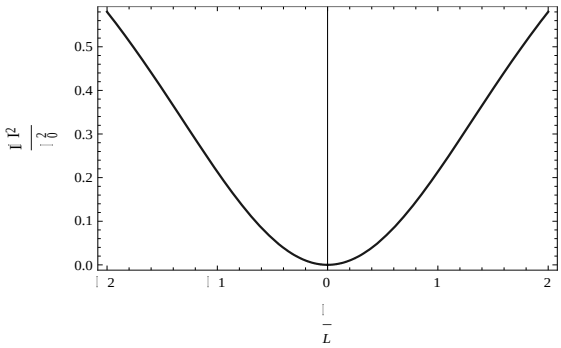

Figure 29: Dark soliton for $L = 2$ *corresponding to* $\omega/\omega_p = .17$, *at* $\tau = 0$.

IV. RESULTS AND DISCUSSIONS

Thus, we analyze the optical properties of the negative index materials (NIMs) under external electromagnetic (EM) fields of intense laser radiation, their linear and nonlinear resonant frequencies, and the propagation of EM fields through NIMs near the resonant region. With the data available, the linear resonant frequency (eigenfrequency) of SSR is found to be 1.45 THz and the magnetic frequency to be 1.87 THz. The resonant frequency and the magnetic frequency creates the frequency band within which the dielectric permittivity and the magnetic permeability simultaneously are negative, which is the main criteria of NIMs. Thus, the founded frequency band is a narrow band. Analyzing Eq.(10) and Eq.(11), it is found that the frequency band becomes more narrower with the increasing intensities of the EM fields of the propagating

wave. Eq.(14) shows that that the magnetic frequency shifts towards the linear resonant frequency with the increase of field intensity. We solve Eq.(17) to find the relation between the nonlinear resonant frequency with the intensity of the wave's magnetic field. With the increasing magnetic field intensity, Eq.(18) shows that the nonlinear resonant frequency goes below the linear resonant frequency in the case of focusing nonlinearity, while it goes up in the case of defocusing nonlinearity . A system of coupled equations [Eq.(25) and Eq.(26)] describes the EM fields propagation through NIMS. From these equations, in the high frequency response, we find the the nonlinear field dependent dispersion relation defined by the Eq. (34). The group velocity of the corresponding wave is defined by the Eq. (35) which shows that the frequency band for wave propagation is more narrowed down with the increase of the field intensities.

In the low frequency response, using the reductive pertubation method, we obtain a coupled [(Eq.(40) and Eq.(41)] nonlinear Schrödinger (NLS) equations . The dispersion coefficient and the nonlinear coefficients of the NLS equations are investigated within the frequency band of NIMs. Considering the same intensities of electric and magnetic fields of the wave, the coupled system is solved, which predicts the propagation of bright and dark solitons through NIMs before and after some critical frequency within the band. Eq.(45) defines the critical frequency, the analysis of which shows that it goes to the linear resonant frequency with the increase of field intensities. The bright soliton is a fast mode which is modulationally unstable. The growth rate of the instability is calculated and it is shown by Eq.(58). Solitons pulse widths are also investigated within the frequency band, which shows that they are more narrower at the resonant frequency and they become wider away from the resonant region. The dark soliton is a slow mode which is modulationally stable.

V. CONCLUSION

To summarize, we have investigated the nonlinear propagation of a terahertz laser radiation in the resonant region of a negative index meta-materials. It is found that the negative refractive index of the meta-material is maintained within a narrow band of frequencies, which is more narrowed down with the increase of field intensities of the propagating wave. The nonlinear resonant frequency of the split ring resonator depends on the intensity of the wave, and it goes below the linear resonant frequency in the case of focusing nonlinearity, while it goes up in the case of defocusing nonlinearity. The nonlinear field dependent dispersion relation and the corresponding group velocity determined in the high frequency response, show that the frequency band of the wave propagation is more narrowed down with the increase of field intensities. The coupled nonlinear Schrödinger equations describing the propagation of the wave in the slow response, predicts the propagation of bright solitons and dark solitons before and after a critical frequency determined by the field intensities within the frequency band. The bright soliton is a fast mode and it is modulationally unstable. The growth rate of the instability is calculated. The dark soliton is a slow mode and it is modulationally stable. Solitons pulse widths are more narrower at the resonant frequency and they become more wider away from the resonant region. Results obtained in this investigation may have some applications in meta-materials using SRR with the negative refractive index in the terahertz spectrum and in photonic crystals, which are to be investigated in near future.

ACKNOWLEDGEMENT

This work has been supported by the Ministry of Education of the Government of Bangladesh under Grants for Advanced Research in Science: MOE.ARS.PS.2011. No.-86. Thanks to Professor Mohammad Zahidur Rahman for encouraging the publication of the research paper on advanced materials in BRAC University Journal.

REFERENCES

1. V. G. Vaselago, *The electrodynamics of substances with simultaneously negative values of* ε , μ. Sov. Phys. Usp **10**, 509, 1968, pp. 14-21 [Uspekhi Phis. Nauk, **92** (3), 1967, pp. 519-526].
2. J. B. Pendry, *Negative refraction makes a perfect lens*, Phys. Rev. Lett, **85**,2000, pp. 3966-9.
3. D. R. Smith, W. J. Padilla, D. C. Vier, S. C. Nemat-Nasser, S. Schultz, *Composite medium with simultaneously negative permeability and permittivity*, Phys. Rev. Lett., **84**, 2000, pp. 4184-4189.

4. S. Linden, C. Enkirch, M. Wegner, J. Zhou, T. Koschny, C. M. Soukoulis, *Magnetic response of metamaterials at 100 terahertz*, Science, **306**, 2004, pp. 1351-1353.

5. P. V. Parimi, W. T. Lu, P. Vodo, S. Sridhav, *Photonic crystal: Imaging by flat lense using negative refraction*, Nature, **426**, 2003, p. 404.

6. E. Cabuku, K. Aydin, E. Ozbay, S. Foteinopoulu, C. M. Soukoulis, *Subwavelength resolution in a two-dimensional photonic crystal based superlens*, Phys. Rev. Lett**, 91**, pp. 207401-1 - 207401-4.

7. K. C. Huang, M. C. Povinelli, J. D. Joannopoulos, *Negative effective permiability in polaritonic photonic crystals*, Appl Phys. Lett., **85**, 2004, pp. 543-545.

8. K. S. Novoselov, A. K. Gleim, S. V. Morozov, D. Jiang, Y. Zang, S. V. Dubonos, I. V. Grigorieva and A. A. Firsov, *Electric Field effect in atomically thin carbon films*, Science, **306**, 2004, pp. 606-669.

9. A. K. Geim, *Graphene: Status and Prospects, Science*, **324**, 2009, pp. 1530-1534.

10. A. R. Wright, X. G. Xu, J. C. Cao and C. Zhang, *Strong nonlinear optical response of graphene in the terhertz regime*, Appl. Phys. Lett. **95**, 2009, pp. 072101-1 - 072101-3.

11. K. L. Ishikawa, *Nonlinear optical response of graphene in time domain*, Phys. Rev. B **82**, 2010, pp. 201402-1 - 201402-4 (R).

12. E. Hendry, P. J. Hale, J. Moger, A. K. Savchenko and S. A. Mikhailov, *Coherent nonlinear optical response of graphene*, Phys. Rev. Lett. **105**, 2010, pp. 097401-1 - 097401-4.

13. C. M. Soukoulis, M. Kafesaki, E. N. Economou, *Negative Index Materials: New Frontiers in Optics*, Adv. Mater**, 18**, 2006, pp. 1941-1952.

14. I. Kourakis and P. K. Shukla, *Nonlinear propagation of electromagnetic waves in negative refraction index composite materials*, Phys. Rev. E **72**, 2005, pp. 0166261-1 - 0166261-4.

15. A. A. Zharov, I. V. Shadrivov and Y. Kivshar, *Nonlinear properties of left-handed metamaterials, Phys. Rev. Let.*, **91**, 2003, pp. 037401-1 - 037401-4.

16. G. I. Melikidze, J. A Gil, A. D. Patarya, *The spark associated soliton model for pulsar radio emission*, Astrophys. J. **544**, 2000, pp.1081-1097.

17. U. A. Mofiz and M. R. Amin, *Langmuir dark solitons in dense ultrarelativistic electron-positron gravito plasma in pulsar magnetosphere*. Astrophys. Space Sci. **345**, 2013. pp.119-124.

18. N. Lazarides and G. P. Tsironis, *Coupled nonlinear Schrödinger field equations for electromagnetic wave propagation in nonlinear left-handed materials.* Phys. Rev. E, **71**, 2005, pp. 036614-1-4.

19. C. L. Nam, *Derivation of nonlinear Schrödinger equation for electrostatic and electromagnetic waves in fully relativistic two-fluid plasmas by the reductive perturbation method*. Phys. Plasmas **19**, 2012, pp. 082303-1 - 082303-13.

20. A. Hasegawa, *Plasma Instabilities and Nonlinear Effects (Springer, Berlin)*, 1975 .

21. U. A. Mofiz, *On the generation of large amplitude spiky soliton by ultralow frequency earthquake emission in the Van Allen radiation belt*, Phys. Plasmas, **13**, 2006, pp. 082901-1 - 082901 -10.

22. T. Cattert, I. Kurakis and P. K. Shukla, *Envelope solitons associated with electromagnetic waves in a magnetized pair plasma*. Phys. Plasmas **12**, 2005, pp. 012319-1 - 012319-6.